

Decentralized Control Using Wireless Signal Communication for Solid-state Transformer with Cascaded Chopper Cell

Keita Ohata
Dept. Science of Technology Innovation
Nagaoka University of Technology
Nagaoka, Japan
keita_ohata@stn.nagaokaut.ac.jp

Masakazu Adachi
Dept. Electrical, Electronics, and Information Engineering
Nagaoka University of Technology
Nagaoka, Japan
m_adachi@stn.nagaokaut.ac.jp

Tetsunori Kinoshita
Dept. Electrical, Electronics, and Information Engineering
Nagaoka University of Technology
Nagaoka, Japan
kinoshita_t@stn.nagaokaut.ac.jp

Koki Yamanokuchi
Dept. Electrical, Electronics, and Information Engineering
Nagaoka University of Technology
Nagaoka, Japan
koki_yamanokuchi@stn.nagaokaut.ac.jp

Shunsuke Takuma
Dept. Science of Technology Innovation
Nagaoka University of Technology
Nagaoka, Japan
takuma_s@stn.nagaokaut.ac.jp

Keisuke Kusaka
Dept. Electrical, Electronics, and Information Engineering
Nagaoka University of Technology
Nagaoka, Japan
kusaka@vos.nagaokaut.ac.jp

Jun-ichi Itoh
Dept. Science of Technology Innovation
Nagaoka University of Technology
Nagaoka, Japan
itoh@vos.nagaokaut.ac.jp

Abstract— This paper proposes a novel decentralized control method and controllers on cells, which communicate with the main controller using Bluetooth communication, for a medium voltage solid-state transformer (SST) with multiple chopper cells. SST requires a considerable number of signal lines between the main controller and each cell in order to communicate the amount of information such as detected DC voltage, current, fail, and commands. The proposed control system with wireless communication is effective in reducing the number of signal lines. Moreover, the proposed control method allows only low-speed communication and uses only a few parameters to be exchanged between the main controller and each cell controllers because the instantaneous values are not required for the control in the proposed method. The validity of the proposed method is demonstrated with a 3-kW prototype. From the experimented results, the input-current imbalance is reduced from 24.6 % to 5.46 %, where total harmonic distortion is less than 3%.

Keywords— *solid-state transformer, multi-port converter, balancing control, wireless signal communication*

I. INTRODUCTION

Solid-state transformers (SSTs) have been attracted in the field of DC distribution systems as a front-end converter for data centers. SST typically consists of multiple small-capacity converters connected in series or parallel [1–6]. The advantages of the multiple cell topology are; availability of use of low-voltage devices, scalability for power capacity and voltage.

The multiple cell topology requires a large number of the signal lines between the main controller and each cell. The signal lines among cell controllers and the main controller are necessary to control the voltages, currents of each cell, and

overall systems coordinately. A great deal of wire connection typically decreases the maintainability of SSTs.

In order to reduce the number of signal lines, decentralized control methods in which each cell independently operates, have been proposed in the previous study [7]. These studies have improved the maintainability of SSTs. However, there are still many signal lines between the cells and the main controller. Thus, a further decrease in the signal lines is required for maintainability and workability.

In order to solve the above problems, a distributed control method with wireless signal communication has been proposed [8–9]. References [8–9] show that high-speed feedback is not required for signals such as detected signal lines, control signal lines, and gate drive signal lines from the cell controllers to the main controller. However, the decentralized control has not experimentally demonstrated [8–9].

This paper experimentally clarifies the proposed decentralized control using the wireless signal communication for SST with cascaded chopper cells. The new contribution of this paper is that the validity of the Bluetooth wireless communication is demonstrated for the cell controller in SST system even if the Bluetooth wireless communication has long delay time. In the rest of the paper, first, the configuration and advantages of the SST with the proposed decentralized control methods are explained. Second, the operation of the decentralized control is described. Finally, the experimental results of the operating SST by the wireless communication are mentioned. Furthermore, the practical test for the wireless communication under the magnetic field from the power converters is verified, as an appendix.

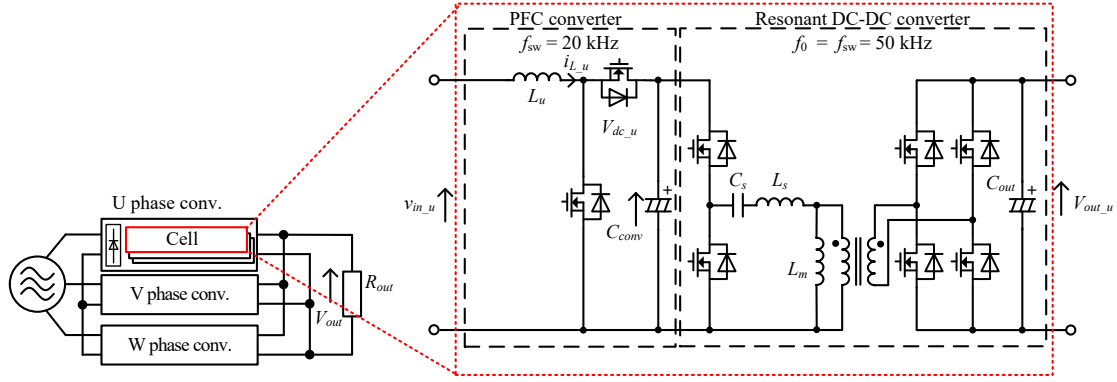


Fig. 1. Solid-state transformer with simple cascaded chopper cells.

II. CIRCUIT TOPOLOGY

Figure 1 shows the circuit configuration of SST with the cascaded chopper cells. The SST is operated as three single-phase AC-DC converters. Each chopper cell consists of the PFC converter and the resonant DC-DC converter. The PFC converters have a role to obtain the sinusoidal input current and unity power factor. The resonant DC-DC converter is employed to achieve galvanic isolation and reduction of switching loss by zero current switchings (ZCS). The zero current switchings are achieved by resonance between the leakage inductance L_s in the high-frequency transformer and the resonant capacitor C_s connected to the primary side of the transformer. Each MOSFET of the high-frequency inverter in the primary side switches at the zero-cross of the current by adjusting the resonant frequency and the switching frequency.

III. PROPOSED CONTROL SCHEME

Figure 2 shows the block diagram of the proposed decentralized control with wireless communication [7]. The control system is separated into the main controller and the cell controllers.

The main controller calculates the averaged current based on the detected current of each phase received from the detection circuit. Afterward, the main controller transmits a output voltage command V_o^* and averaged current I_0 to each cell. To summarize

the role of the main controller, the main controller is only for calculating the averaged value and communicating with each cell. Thus, it is possible to employ slow speed microcomputer, which is desirable from a cost point of view. The averaged current I_0 is given by

$$I_0 = \frac{I_u + I_v + I_w}{3} \quad (1),$$

where I_0 is the averaged current of the three-phase current calculated every few milliseconds.

The function of the cell controller in communication with the main controller and secondary voltage control with input phase current control in the minor-loop. Besides, the secondary voltage control scheme employs the droop control and current balancing control in order to prevent diffusion of input current and power-sharing.

A. Droop control

Figure 3 (a) and (b) show the equivalent circuit models of SST, focusing on the output of the cells, which are connected in parallel at a DC bus. Each cell connected to the DC bus individually controls the output voltage with feedback control. However, the interactions of the voltage feedback control between each cell lead a weak system performance or may drive

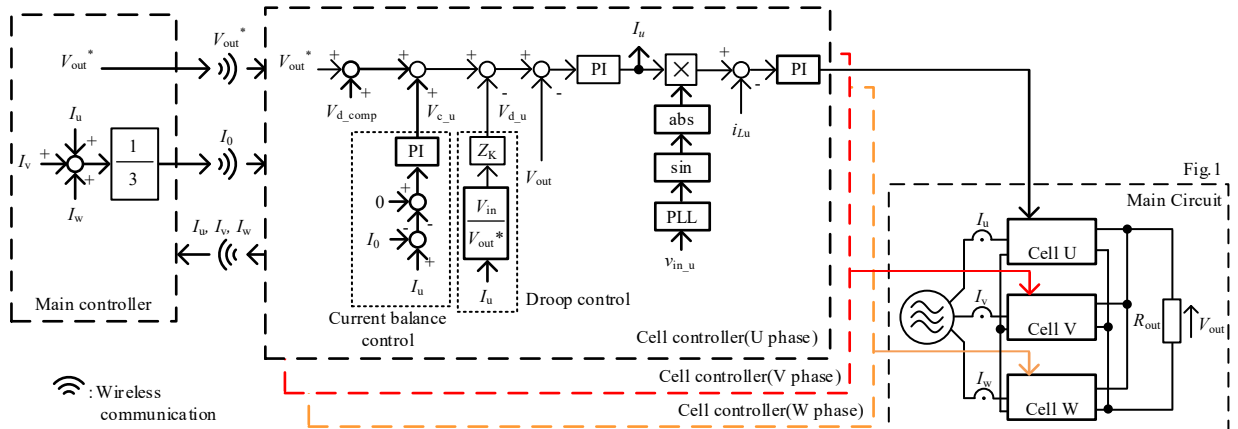


Fig. 2. Block diagram of proposed decentralized control with wireless communication.

the system to instability. The imbalance of the output voltage causes a rush current. The difference in voltage is caused by two reasons; The first reason is a gain error of amplifier for a current sensor. The second is the temperature drift of the current sensor and the detection circuit.

In order to solve the above problems, the virtual resistors in order to eliminate inrush current are implemented in series to each output voltage source by the droop control, as shown in Fig. 3 (b). In other words, the virtual resistors mitigate the mutual interference of the voltage feedback control of each cell in exchange for the high-dynamic response and the steady-state deviation on the output voltage. The drop voltage of virtual resistor V_{d_u} , V_{d_v} , V_{d_w} are given by

$$V_{d_u} = \frac{V_{in}}{V_{out}^*} Z_K I_u \quad (2),$$

$$V_{d_v} = \frac{V_{in}}{V_{out}^*} Z_K I_v \quad (3),$$

$$V_{d_w} = \frac{V_{in}}{V_{out}^*} Z_K I_w \quad (4),$$

where V_{in} is the input rectified voltage, V_{out}^* is the output voltage command. Thus, the controller adds feedforward to this value as V_{d_comp} .

B. Current balance control

The droop control prevents uncontrollable current, as explained in the previous section. Note that implementing only the droop control might result in imbalanced of the input phase current in each cell. Thus, the proposed control method is employed the input phase current balance control strategy to eliminate the current imbalance. As shown in Figure 2, the manipulated variables V_{c_u} , V_{c_v} , V_{c_w} are added to the output voltage command in order to make the detected peak value of the phase current following the averaged current in the input phase current balance control. The notable feature of the strategy of the input current balance control is that a fast response is not

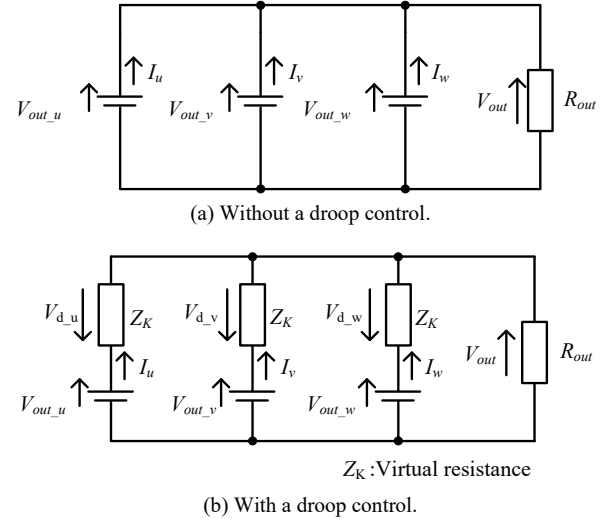


Fig.3. Equivalent circuit models of SST focusing on the output of the cells.

required. In other words, high-speed communication and the high computing power of the main controller are not necessary.

Besides, a conventional decentralized system controls the current of each cell by the main controller. The conventional method requires a fast response. For this reason, only the proposed control scheme accepts the inclusion of wireless communication.

IV. STRUCTURE OF EXPERIMENTAL CIRCUIT

Figure 4 shows the experimental configuration with wireless communication. The proposed control method does not require high-speed communication between the main controller and the cell controllers, as mentioned in chapter III. Note that this communication standard is not only Bluetooth specification but also several communications technologies such as Wi-Fi, ZigBee, or sub-GHz wireless can be used as the wireless communication method in cells.

A. Main controller

Figure 5 (a) shows a photograph of the main controller for the experimental circuit, including decentralized control using a wireless module. The main controller consists of DSP, FPGA, a bus controller, and three Bluetooth modules (Microchip,

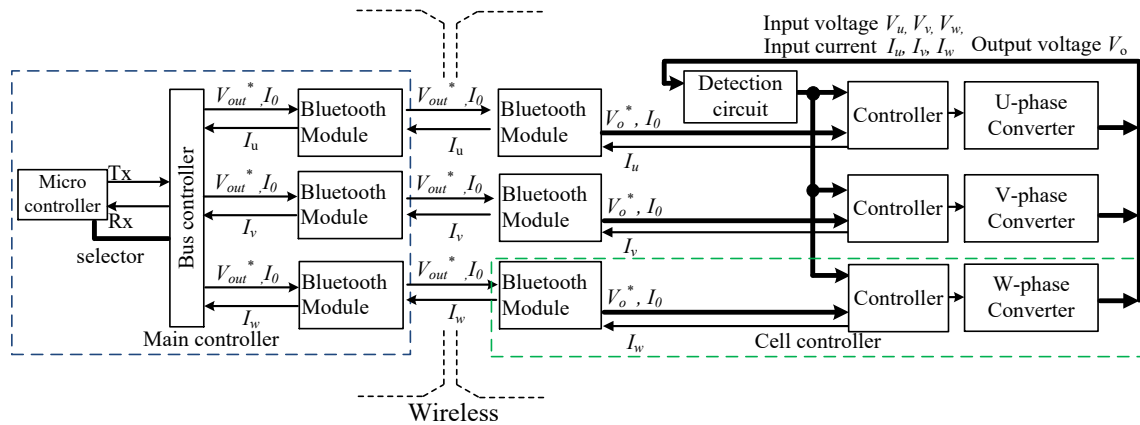


Fig. 4. Experimental configuration with wireless communication.

RN4020). The controller transmits output voltage command V_o^* and the average value of phase current I_0 . Moreover, the main controller receives each phase current I_u (or I_v or I_w), the main controller calculates the average value of phase current by (1). The wireless module accepts only one to one communication. Hence, three modules are installed on the main controller. The number of wireless communication modules on the main controller side is reduced when using a wireless communication module capable of 1-to- N communication. The communication is based on Universal Asynchronous Receiver / Transmitter (UART), 115,200 bps. In the proposed control method, a general-purpose controller can be applied as the main controller because the calculation of the main controller is only (1). Table I lists the specification of the wireless module. The main controller is applied to the same controller of the cell for simplicity.

B. Cell controller

Figure 5 (b) shows a photograph of the cell controller for the experimental circuit. The cell consists of a Bluetooth module, a detection circuit, a controller, and the main converter. The controller controls the output voltage and input current based on the received data V_o^* and I_0 .

C. Structure of wireless communication

A data structure of transmitted and received data is five bytes per parameter. The proposed method uses two parameters in a transmitting process from the main controller to the cell controller and one parameter in another transmitting process from the cell to the main. Thus, the number of byte per control cycle is 45 bytes. The measurement of required time for the communication cycle is 270 ms in the condition of section V. The cycle is decided by the communication time, the delay time, and the processing overhead in the wireless module.

V. EXPERIMENTAL RESULTS

In this chapter, the experimental results of the proposed control scheme is introduced. Table II lists the experimental conditions.

A. Steady-state

Figure 6 shows the input current i_u , i_v , and i_w waveforms and the output voltage V_o waveform at the steady-state with or without the proposed method when $V_o^* = 400$ V, and $P = 1.5$ kW. The phase current is high-distorted, and power-sharing is ununiformed when the droop control and the current balance

control are disabled in Fig. 6(a). Whereas, each phase current is controlled in a sinusoidal shape, and the amplitudes are matched in Fig. 6(b). The input current THD of each phase is 3 % or less. The input-current imbalance rate is reduced from 24.6 % to 5.46% compared to without the proposed method. Here, the imbalance rate of the input current is defined as

$$\varepsilon_{\text{current_err}} [\%] = \left| \max \left\{ \frac{I_u - I_0}{I_0}, \frac{I_v - I_0}{I_0}, \frac{I_w - I_0}{I_0} \right\} \times 100 \right| \quad (5).$$

B. Transient-response

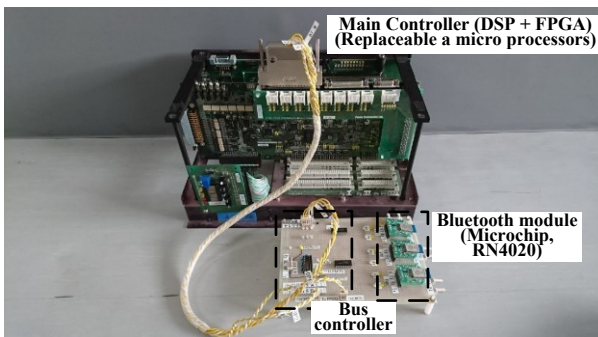
Figure 7 shows the input current i_u , i_v , and i_w waveforms and the output voltage V_o waveform at the transient-state when the output voltage command V_o^* changes from 250 to 400 V. The transient response has a delay about one second by wireless communication. The overshoot occurs at the change of output voltage command on each cell controller. After 1.2 s, the input

TABLE I. Specification of wireless module.

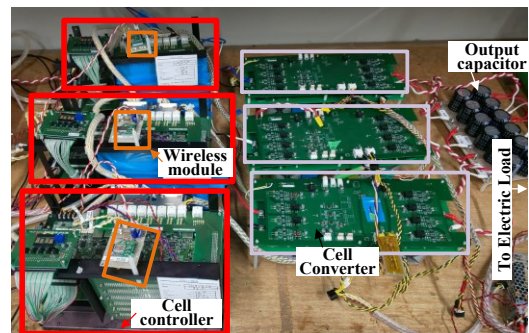
Corporation	Microchip
Communication standard	Bluetooth ver. 4.1
Product name	RN4020
Module size	13.4 mm × 25.8 mm × 2 mm
Maximum speed	240 kbps
Allowable transmission distance	20 m

TABLE II. Experimental Conditions.

Quantity	Symbol	Value
Input voltage	V_{in}	283 V (200√3 V)
Rated output power	P	3 kW
DC-link capacitance	C_{conv}	48 μF
Output capacitance	C_{out}	2040 μF
Input inductance	L	3 mH (%Z=2.3 %)
Switching frequency (PFC)	f_{sw}	20 kHz
Resonant frequency (Resonant DC-DC converter)	f_o	50 kHz
Angular frequency of ACR	ω_{ACR}	6000 rad/s
Angular frequency of AVR	ω_{AVR}	50 rad/s
Proposal gain of current balance control	K_c	2.0



(a) Main controller.



(b) Cell controllers and cell converters.

Fig. 5 Photograph of experimental circuit including decentralized control using wireless module.

current converges by the proposed control with wireless communication.

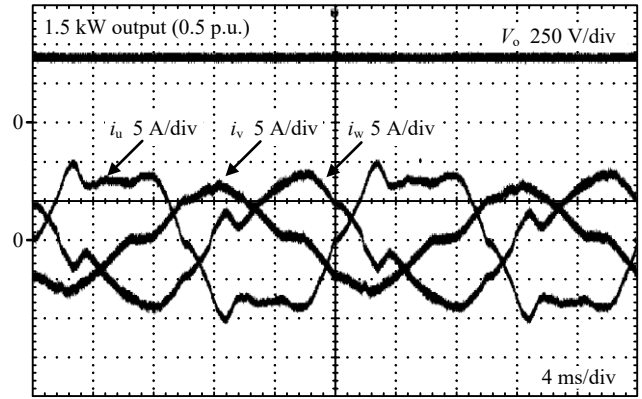
VI. CONCLUSION

In this paper, the decentralized control method using wireless communication is employed for the control system of SST. The proposed control system is characterized by the droop control and the current balance control. These controls are the outer loop of the feedback voltage control. As a result, a simple configuration and wireless communication are available when the circuit scale is increased by using the cascaded chopper cell. In the experimental results of the 3-kW prototype, the input-current imbalance rate is reduced from 24.6 % to 5.46 %, and the input current THD is 3% or less. The compensation for delays of the wireless communication will be considered when the number of cells further increases.

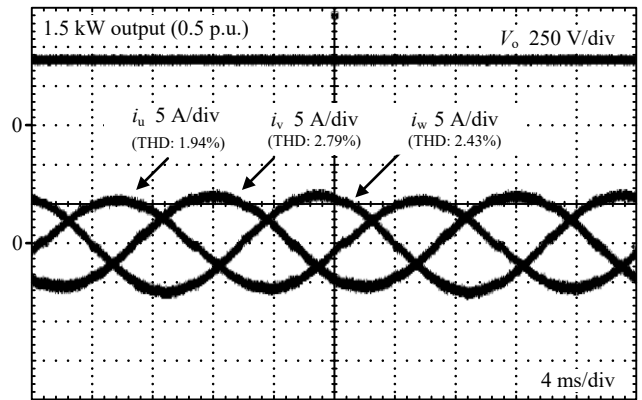
APPENDIX

VII. PRACTICAL TEST FOR WIRELESS COMMUNICATION IN POWER CONVERTERS

In this section, the effect of radiated noise generated by the power converters on the wireless communication module, e.g., the communication error rate, effective speed, and transmission distance, is evaluated. This evaluation is necessary because the communication between the main controller and the cell controller uses the wireless communication module, which is located near the power converter in the proposed circuit. From the aforementioned discussion, the wireless communication module is placed near the three types of power converters, and



(a) Without proposed balance method.



(b) With proposed balance method.

Fig. 6 Waveform at the steady-state with or without the proposed balance method through Bluetooth communication.

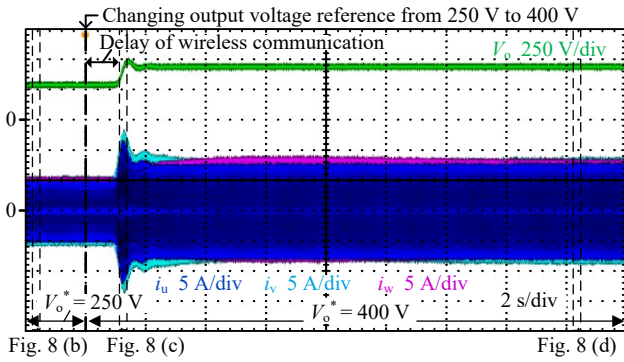
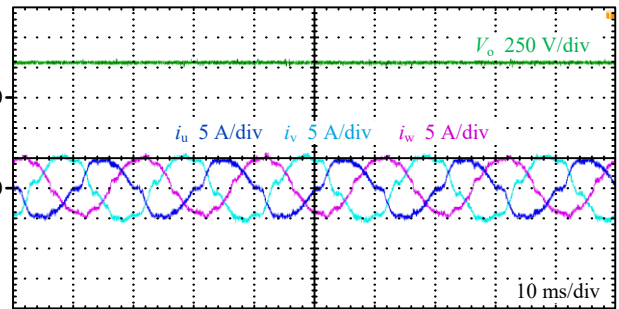


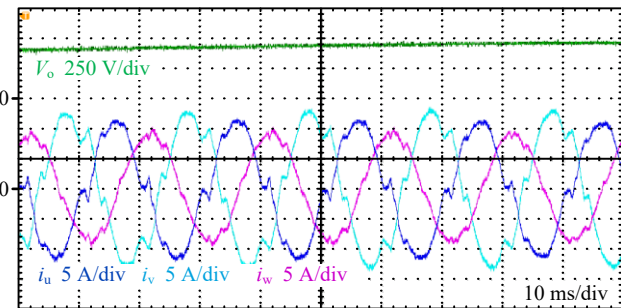
Fig. 8 (b) Fig. 8 (c)

Fig. 8 (d)

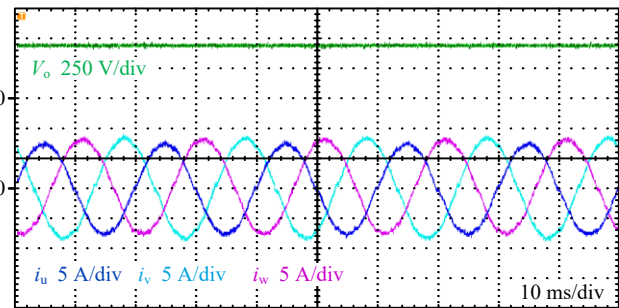
(a) Outline.



(b) Extended Fig. 7(a): Before changing output voltage command.



(c) Extended Fig. 7(a): Overshoot.



(d) Extended Fig. 7(a): After changing output voltage command.

Fig. 7. Waveform at the transient response when change output voltage command from 250 V to 400 V

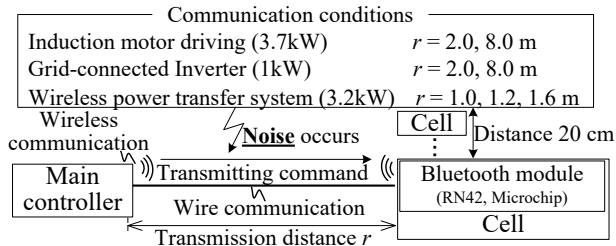


Fig. 8. Outline of experimental environment. Three type of converters are placed away the Bluetooth module from 20 cm as noise source.

TABLE III. Specification of wireless module at the practical test.

Manufacture	Microchip
Communication standard	Bluetooth ver. 2.1 + EDR
Product name	RN42
Module size	13.4 mm × 25.8 mm × 2 mm
Maximum speed	240 kbps (Slave), 300 kbps (Master)
Allowable transmission distance	20 m

the effective communication speed and error rate of communication are evaluated.

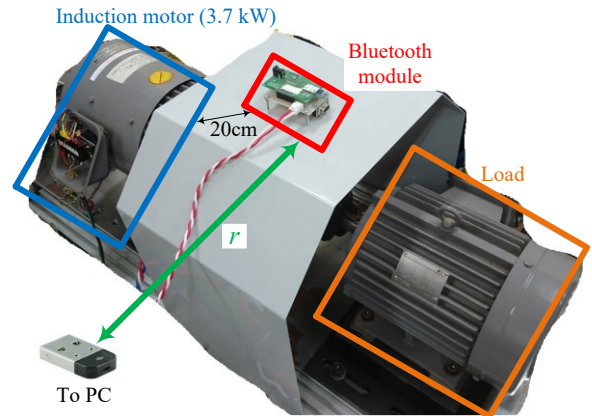
Figure 8 shows the outline of the experimental environment for measuring the effect of radiated noise from the power converters on the Bluetooth module. Note that the experiment was conducted using the Bluetooth module RN42 (Microchip). Table III lists the specification of wireless module RN42.

Figure 9 shows the photograph for the experimental environment. The three types of converters are placed away from the Bluetooth module from 20 cm as a noise source. In addition, the Bluetooth communication distance is changed from 2 m to 8 m to evaluate the effective speed against the transmission distance.

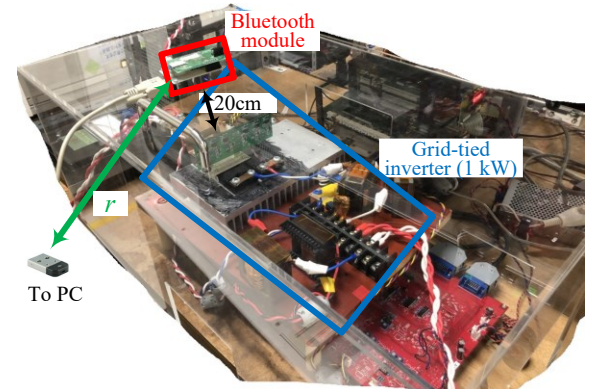
Figure 10 shows the relationship between the effective speed and transmission distance. Bluetooth communication operates at a communication speed of 250 bit / s to 400 bit / s near power converters. Moreover, in the comparison between transmitted data and received data, the error rate is 0% under all conditions. The experimental results indicate that the communication errors do not occur even when the wireless communication module is operated nearby 3.2-kW wireless power transfer system, which emits much radiation noise, a 1-kW grid-tied inverter, and a 3.7-kW induction motor. From experimental results, the Bluetooth module is suitable for the communication tool of some power converters.

REFERENCES

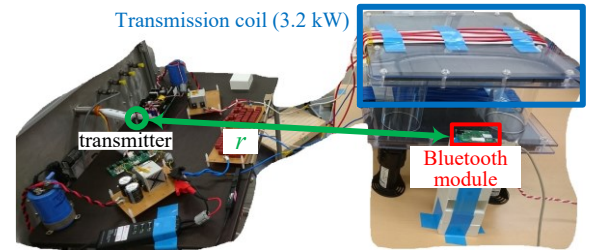
- [1] C. Liu et al., "An Isolated Modular Multilevel Converter (I-M2C) Topology Based on High-Frequency Link (HFL) Concept," IEEE Transactions on Power Electronics, vol. 35, no. 2, pp. 1576-1588, Feb. 2020.
- [2] J. E. Bosso, M. Llomplat, G. G. Oggier and G. O. García, "Evaluation of DC-AC Single-Phase Solid-State Transformers", in IEEE Latin America Transactions, vol. 17, no. 05, pp. 708-717, May 2019.
- [3] H. Chen, A. Prasai, R. Moghe, K. Chintakrinda and D. Divan, "A 50-kVA Three-Phase Solid-State Transformer Based on the Minimal Topology: Dyna-C," IEEE Transactions on Power Electronics, vol. 31, no. 12, pp. 8126-8137, Dec. 2016.



(a) Induction motor (3.7 kW).



(b) Grid-tied inverter (1 kW).



(c) Wireless power transfer system (3.2 kW).

Fig. 9. Photograph of the experimental environment for measuring the effect of radiated noise from some power converters on the Bluetooth module.

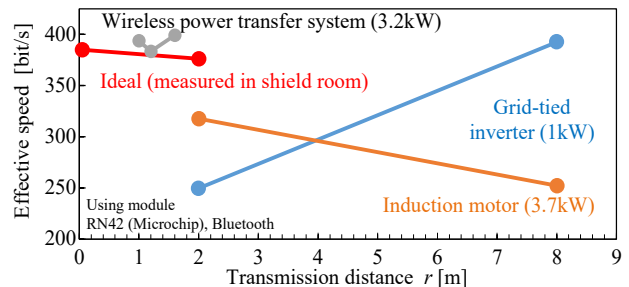


Fig. 10. Relationship between effective speed and transmission distance when the wireless communication module is operated nearby power converters.

- [4] Mizuki Nakahara, Yuki Kawaguchi, Kimihisa Furukawa, Mitsuhiro Kadota, Yuichi Mabuchi, Akihiko Kanoda, "Development of a Control Method for LLC Converter Utilized for Input-Parallel-Output-Series Inverter System with Solid-State Transformers", IEEJ Journal of Industry Applications, vol.8, no. 5, pp. 652-659, Jul 2019.
- [5] Yusuke Hayashi and Tamotsu Ninomiya "Highly Scalable Sensorless Multicellular AC-DC Transformer (ADX) for the DC Distribution System in Data Centers," IEEJ J. Industry Applications, vol. 7, no. 6, pp. 479-487, 2018.
- [6] Jun-ichi Itoh, Kazuki Aoyagi, Keisuke Kusaka, Masakazu Adachi, "Development of Solid-state Transformer for 6.6-kV Single-phase Grid with Automatically Balanced Capacitor Voltage", IEEJ Journal of Industry Applications, vol.8, no.5, pp. 795-802, Sep 2019.
- [7] J. Nie, L. Yuan, Q. Gu, J. Sun and Z. Zhao, "A Coordinate and Distributed Control Scheme for Multilevel and Multi-Stage Medium Voltage Solid State Transformer," 2018 International Power Electronics Conference (IPEC-Niigata 2018 -ECCE Asia), Niigata, Japan, 2018, pp. 2963-2968.
- [8] Masakazu Adachi, Keisuke Kusaka, Jun-ichi Itoh, "Multi-Modular Isolated Three-Phase AC-DC Converter for Rapid Charging with Autonomous Distributed Control", EVS 31 & EVTeC 2018, Kobe, Japan, 2018
- [9] K. Ohata, M. Adachi, K. Kusaka and J. Itoh, "Three-phase AC-DC Converter for EV Rapid Charging with Wireless Communication for Decentralized Controller," 2019 10th International Conference on Power Electronics and ECCE Asia (ICPE 2019 - ECCE Asia), Busan, Korea (South), 2019, pp. 3033-3039.